Supplementary

A. Vertical land motion statistics

Table A.1: Statistics of InSAR-derived vertical land motion within the administration boundary of each coastal city. Negative velocity refers to land subsidence.

No.	Coastal City	Country	95th Percentile of Negative Velocities (mm/year)	Median of Velocities (mm/year)
1	Tianjin	China	-42.9	-5.7
2	Ho Chi Minh City	Vietnam	-42.7	-16.2
3	Chittagong	Bangladesh	-37.4	-11.8
4	Yangon	Myanmar	-30.8	-3.9
5	Jakarta	Indonesia	-26.1	-4.4
6	Ahmedabad	India	-22.7	-4.7
7	Istanbul	Turkey	-19.4	-6.2
8	Houston	USA	-17.3	-2.8
9	Lagos	Nigeria	-17.2	-1.4
10	Manila	Philippines	-17.0	-1.7
11	Surat	India	-16.5	-4.7
12	Shanghai	China	-14.1	-2.5
13	Guangzhou	China	-13.6	-1.9
14	Suzhou	China	-13.2	-1.4
15	Hong Kong	China	-13.0	-1.1
16	Fukuoka	Japan	-12.5	-2.8
17	Sao Paulo	Brazil	-12.2	-5.7
18	Dhaka	Bangladesh	-12.0	-0.3
19	Abidjan	Côte d'Ivoire	-11.6	-1.9
20	Chennai	India	-11.3	0.4
21	Barcelona	Spain	-10.8	-0.6
22	Foshan	China	-10.7	-1.7
23	Qingdao	China	-9.8	-3.6
24	Dalian	China	-9.3	-0.1
25	Mumbai	India	-8.9	-0.9
26	London	England	-8.8	-0.3
27	Kolkata	India	-8.3	-1.9
28	Nanjing	China	-8.2	1.1
29	Luanda	Angola	-7.6	0.6
30	Alexandria	Egypt	-7.4	0.0
31	Bangkok	Thailand	-7.0	0.0
32	Hangzhou	China	-7.0	-0.9
33	Rio de Janeiro	Brazil	-6.9	-2.4
34	Singapore	Singapore	-6.9	-1.4
35	Karachi	Pakistan	-6.2	-0.2
36	Osaka	Japan	-6.2	-1.7
37	Saint Petersburg	Russia	-5.7	-1.7
38	Kuala Lumpur	Malaysia	-5.4	1.2
39	Dongguan	China	-5.1	-0.1
40	Dar es Salaam	Tanzania	-5.0	-0.5
41	Los Angeles	USA	-4.6	-0.7
42	Miami	USA	-4.5	-0.1
43	Lima	Peru	-4.4	-0.6
44	Philadelphia	USA	-4.3	-0.2
45	New York	USA	-3.9	-0.6
46	Buenos Aires	Argentina	-3.7	-0.3
47	Seoul	South Korea	-3.3	-0.2
48	Pune	India	-2.8	-0.5
49	Tokyo	Japan	-2.7	-0.7
50	Washington, D.C.	USA	-2.6	0.6
51	Nagoya	Japan	-2.4	0.2

B. InSAR time series analysis

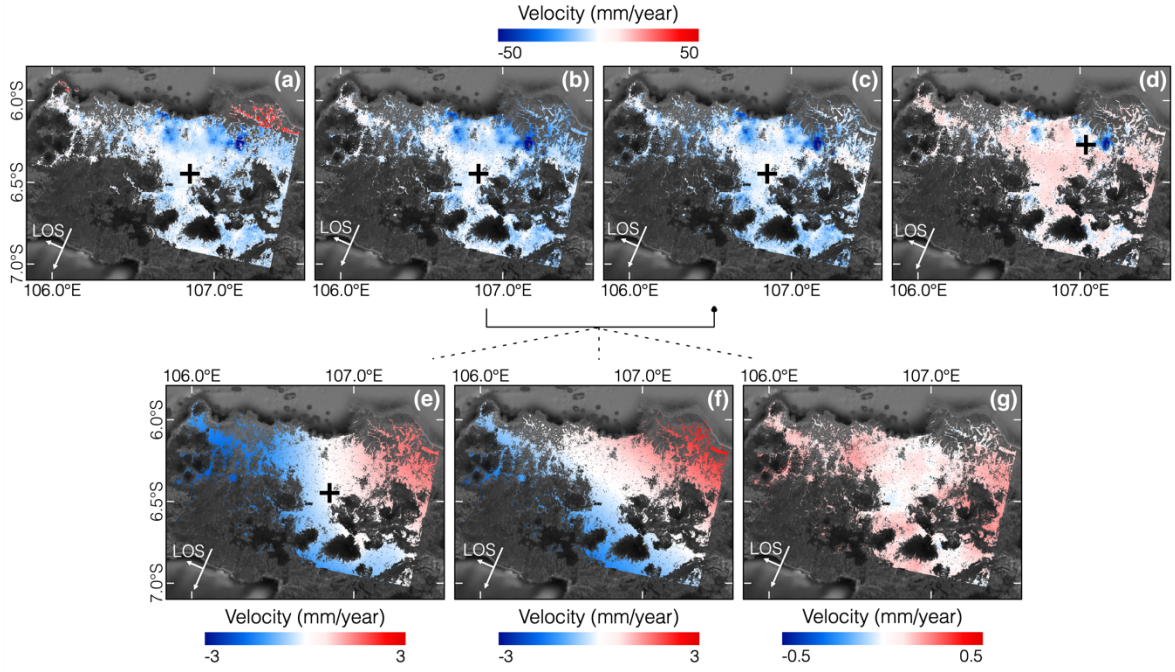

Figure B.1: Effects of InSAR time series processing parameters and corrections. The panels show InSAR line-of-sight velocities over Jakarta, Indonesia **a.** before phase unwrapping error correction, **b.** after phase unwrapping error correction, **e.** contributed from tropospheric delay correction, **f.** contributed from linear phase deramping, **g.** contributed from topographic residual correction, **c.** after corrections from **e** to **g** are applied, and **d.** identical to **c** but using a random pixel of high coherence for the reference point. The reference point in **a** to **c** was selected through the procedure describe in the Methods. Basemap: Google.

C. Spatial interpolation of InSAR velocities

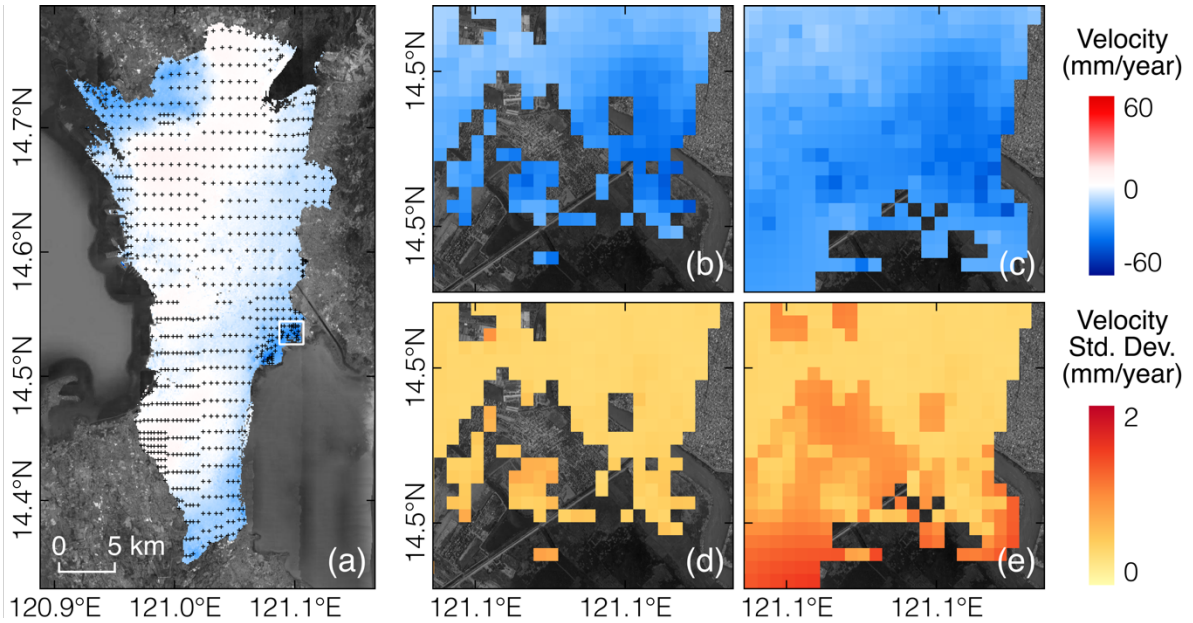

Figure C.1: Kriging with variable uncertainties to fill gaps where InSAR velocities could not be derived from time series analysis – an example in Manila, Philippines. The kriged result is more dependent on data points with lower standard deviations. The panels show **a.** velocities and black crosses indicating the locations of quadtree

subsampled data points used to estimate kriging parameters, **b, d**. data derived from time series analysis only, and **c, e.** data derived from time series analysis with gaps filled with kriged results. Basemap: Google.

D. Localized vertical land motion from InSAR line-of-sight velocities

We illustrate the difference between vertical land motion derived from Sentinel-1 InSAR velocities from a single look direction and from two look directions. The former refers to using observations from either the ascending or descending orbit, and assuming no horizontal land motion when projecting the line-of-sight observations to the vertical due to a lack of viewing geometry. The latter refers to a combination of observations from both ascending and descending orbits to resolve for vertical and horizontal east-west components, and assuming no horizontal north-south motion due to the satellite's near-polar orbit (Eq. 1 in main text). Any deviation of the estimated vertical land motion from the actual vertical land motion increases as horizontal motion increases.

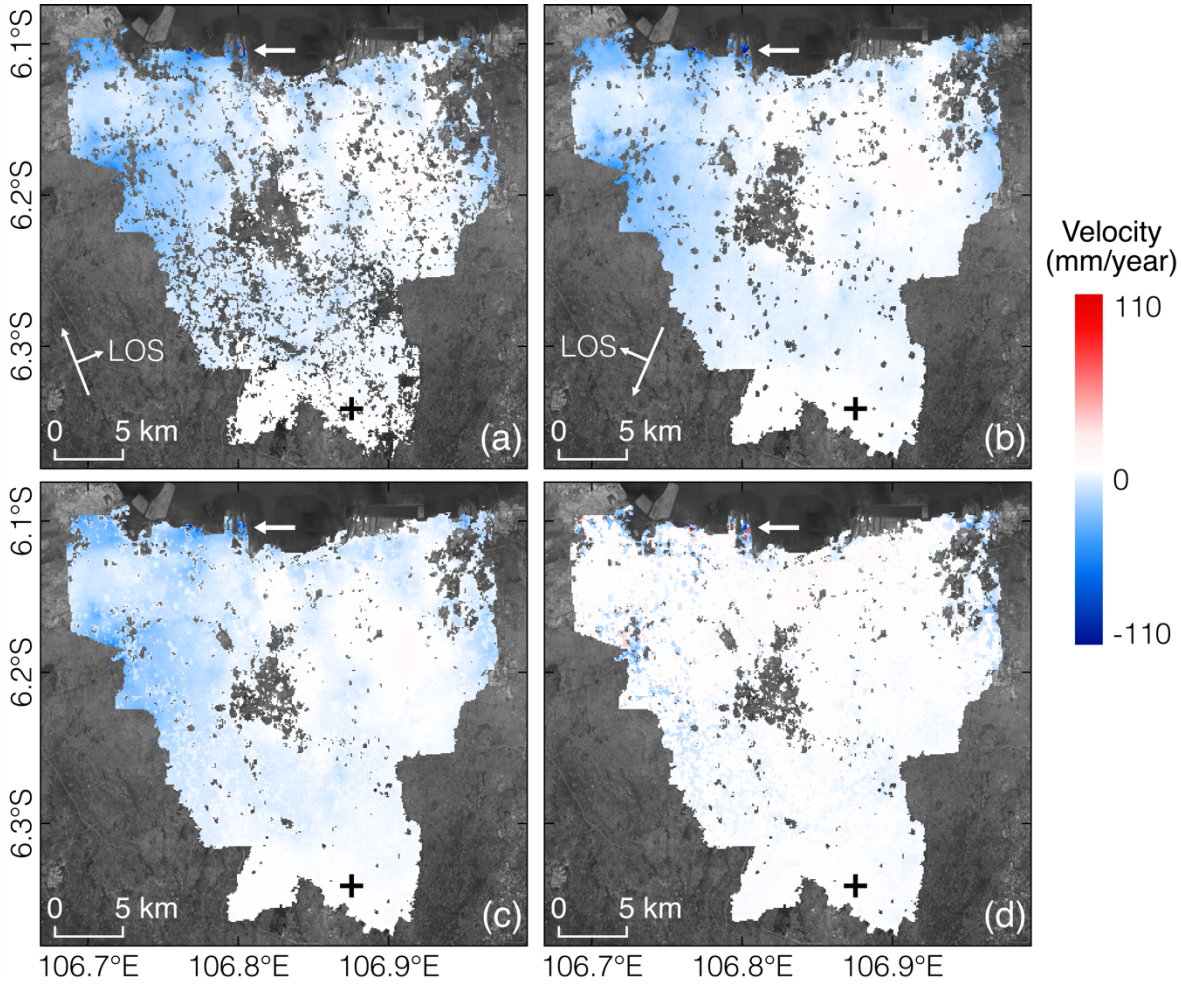

Figure D.1: Comparison of vertical land motion derived from a single look direction and from both look directions combined. The panels show Sentinel-1 InSAR velocities processed within the administrative boundaries of Jakarta, Indonesia in the **a.** vertical direction from an ascending orbit, **b.** vertical direction from a descending orbit, **c.** vertical direction from a combination of both look directions, and **d.** horizontal east-west direction from a combination of both look directions. The thick white arrow indicates the fastest subsiding area. Basemap: Google.

We show an example in Jakarta, Indonesia, where some horizontal land motion may be expected to accompany large vertical land motion due to the presence of rapidly subsiding

areas (Figure D.1). It should be noted that the ascending orbit velocities are noisier and have fewer coherent pixels than that of the descending orbit, likely due to noise from tropospheric delay. The vertical velocities are overall similar across the single-look ascending, single-look descending and double-look cases. At the center of the fastest subsiding area, the single-look ascending, single-look descending, double-look vertical and double-look horizontal east-west velocities are -92 mm/year, -103 mm/year, -94 mm/year and -11 mm/year respectively. Horizontal land motion is still significantly smaller than vertical land motion in the fastest subsiding areas. Thus, InSAR observations from a single look direction were used in this study to produce the global set of vertical land motion for practical reasons.